NUCL SCI TECH (2021) 32:126
https://doi.org/10.1007/s41365-021-00964-1

Simulation results of the online tritiated water measurement system

Rui-Yang Xu[1] · Chun-Hui Dong[1] · Xiao-Qing Mao[2] · Qing-Xian Zhang[1] · Hui Gong[1] · Kai-yong Liao[1] · Zhi-Gang Lu[1] · Liang-quan Ge[1] · Zhi-Yu Gao[2] · Ting-Fang Luo[2] · Qi-Chang Huang[2]

Received: 26 May 2021 / Revised: 9 September 2021 / Accepted: 13 September 2021 / Published online: 18 November 2021

Abstract Currently, the liquid scintillation method is widely used to measure the activity of tritiated water in the primary circuit of nuclear power plants, which leads to the continuous production of radioactive waste during measurement. In addition, the real-time activity information of tritiated water cannot be obtained. To solve this problem, herein we present an online tritiated water measurement method based on plastic scintillators that used the optical transport process in the Geant 4 software toolkit to build a model of plastic scintillation detection for tritiated water. Through simulation, the basic geometric dimensions of the detector were determined. In this dimension, using one detector to measure for 3 h, when the tritiated water activity was 100 Bq/L, its resolution was 16% (16 Bq/L). In addition, calculations were performed for the presence of other background signals to obtain the minimum detectable concentration.

Keywords Tritiated water · Geant 4 · Plastic scintillators · Measurement system

1 Introduction

Tritium is an isotope of hydrogen (^{3}H). It can be found in air, water, food, and all living organisms through isotope exchange with hydrogen in water and organisms [1, 2]. The biological effects caused by the intake of different forms of tritium are significantly different [3]. The solubility of tritium gas in human blood is low, thus the internal radiation dose produced by tritium gas entering the blood is low. However, tritium gas can enter the lungs through breathing, which is an important factor causing internal radiation dose [4]. The harm caused by tritiated water is greater than that caused by tritium gas. Tritiated water can be evenly distributed throughout the human body within 2–3 h, and the radiological harm caused by tritiated water is 2500 times more than that caused by tritium gas [5]. Tritium mainly exists in the form of tritiated water (HTO). There are two ways to produce tritiated water: natural formation and artificial formation; and the amount of artificial tritiated water released is much higher than that of natural tritiated water produced. Currently, governments and related organizations have enacted legislation and promulgated regulations that stipulate the maximum concentration of tritium in drinking water. For example, the U.S. Environmental Protection Agency (EPA) sets a maximum of 740 Bq/L [6] and the EU Council Directive 2013/51/Euratom, establishes a limit of 100 Bq/L [7].

The tritium in the environment originates from both natural formation and artificial formation. The release rate of artificial tritium is higher than that of natural tritium. Artificially released tritium mainly comes from nuclear weapon experiments and reactors [8]. Owing to the prohibition of nuclear testing and the gradual rise of the nuclear power industry, there is an increase in the amount

This work was supported by the National Natural Science Foundation of China (No. 12105029).

✉ Chun-Hui Dong
dongchunhui@cdut.edu.cn

[1] Chengdu University of Technology, Chengdu 610059, China

[2] Nuclear Power Institute of China, Chengdu 610005, China

of tritium released from nuclear power plants. In nuclear power plants, tritiated water is mainly produced in the water coolant and the moderator, and its amount depends on the type of reactor. The Chinese government has proposed requirements for the detection of liquid effluents from nuclear power plants, including tritium as a separate test item and clarified restrictions on tritium emissions. The PWR nuclear power plant continuously generates tritium due to the reaction of boric acid and neutrons in the primary circuit system, and the tritium activity reaches 10^7 Bq/L when operating at a stable power [9]. After processing, the activity of tritium in the liquid effluent was approximately 100 Bq/L. Traditional tritium concentration measurement methods include the β-ray-induced X-rays (BIXS) method [10], calorimetry [11, 12], imaging plate method [13], the liquid scintillation method [14, 15]. The BIXS method is a convenient and non-destructive tritium measurement method. However, because of the low energy of β-rays produced by tritium decay (0–18.6 keV), the intensity of X-rays generated in the material is insignificant, so the detection efficiency of the BIXS method is low. The calorimetry method converts kinetic energy into heat energy in the sample chamber based on β-rays by tritium decay. It calculates the tritium content by measuring temperature change in the sample chamber. However, the small change in the water tritium concentration will cause a small temperature change in the sample room, which will lead to a higher detection limit of this method (approximately 2×10^9 Bq/L), and the measurement time of the calorimetry method is relatively longer. The operation of the imaging plate method is complicated and risky. This method ought to work by exposing the imaging plate to tritium water vapor for up to 24 h before measurement, which poses security risks. Its detection limit is 4×10^6 Bq/L [13], which cannot be used for online measurement of low-concentrated tritiated water. Currently, nuclear power plants widely use offline liquid scintillation methods to measure the concentration of tritiated water. The detection limit of the liquid scintillation method is less than 100 Bq/L, but its shortcomings are obvious. In the actual measurement process, it is necessary to select the type of scintillation liquid according to the specific situation. In addition, the selection of scintillation bottles, the amount of scintillation liquid, the pretreatment of samples, and the holding time will affect the measurement results [16, 17]. It takes approximately two days for a single measurement, which makes it impossible to grasp the tritiated water activity information in the liquid effluent of nuclear power plants in real time. Simultaneously, when the concentration of tritiated water is measured by the liquid scintillation method, liquid waste is produced continuously, which runs counter to the purpose of environmental protection. To solve these problems, this study designs a set of low-activity tritiated water online measurement systems.

2 Detector system

The β-rays produced by tritium decay have a maximum energy of 18.6 keV. Its range in water is only a few microns, and its penetration ability is poor. This leads to a very small number of β-rays that can be detected, which means that the detection efficiency is very low [18]. To improve the detection efficiency of the detector for tritiated water, it is necessary to have a sufficiently large contact area between the tritiated water and the detector. In the initial stage of the detector design, we consider using multiple parallel-arranged fibers to form a detector array. According to the investigation, it was found that the common optical fiber is composed of an internal luminescent medium and an external cladding. The thickness of the external cladding is generally 1–2% of the diameter of the optical fiber. Through Geant 4 simulation, it was found that the range of β-rays produced by tritium decay in water and plastic scintillators is less than 5 μm, which cannot penetrate the cladding of the fiber with the smallest diameter (1 mm) on the market. Because the internal luminescent medium and cladding are formed in one body during the production of the fiber, through investigation, we found that only *SAINT-GOBAIN* sells non-cladding scintillation fibers. Owing to the cost and embargo issues, we propose a technical scheme to increase the contact area by drilling dense boreholes in a cylindrical plastic scintillator. The contact area between the tritiated water and the detector can be increased by increasing the flow channel of tritiated water by drilling boreholes. A structure diagram of the detector is shown in Fig. 1.

The entire detector is divided into three parts: a plastic scintillator, sealing shell, and photomultiplier tubes (PMT). The sealing shell in the middle part of the detector is a PC tube that can be demountable. The number of PC tubes can be added or reduced depending on change in the detector length. Tritium decays to emit β-rays. Some β-rays can reach the plastic scintillator and deposit energy. Subsequently, scintillation photons were produced. The scintillation photons propagate through the plastic scintillator and water; and finally reach the PMT. Then, they are converted into photoelectrons and detected. Considering the size of the photocathode matching the PMT, a cylindrical plastic scintillator with a diameter of 5 cm, which has some water flow channels, was selected. The density of the plastic scintillator is 1.05 g/cm^3, and the ratio of carbon to hydrogen is 1:1.1. The luminescence spectrum is provided by the manufacturer. The peak of the plastic scintillator spectrum is at a wavelength of approximately 420 nm, and

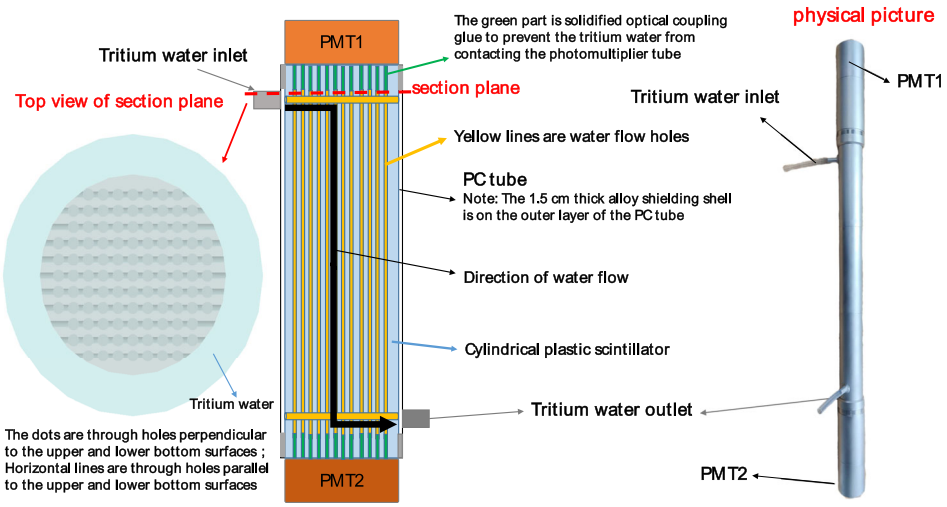

Fig. 1 (Color online) Detector model and physical picture

the light yield is 11250 photons/MeV (the nonlinear problem of the light yield of the plastic scintillator in the low-energy range is not considered here). The decay time of the scintillation photons is 2.4 ns. The entire detector shell adopts the structures of the inner and outer layers. The inner layer uses Teflon material to reflect the scintillation photons, and the outer layer uses an alloy shell to shield the radiation from the background of the environment. Owing to the low energy of the β-rays produced by tritium decay, the number of scintillation photons generated is relatively small. Part of the scintillation photons are lost owing to the self-absorption of the material during the propagation process. Considering the quantum efficiency of the PMT, the number of photoelectrons produced on the PMT is very small. Therefore, two PMTs are used for coincidence measurements to effectively reduce false counting caused by the dark current of the PMT. To improve the detection efficiency of PMT for scintillation photons, PMT selects Hamamatsu R6231-100 with a smaller dark current, larger electron multiplication gain, and higher quantum efficiency. According to the data provided by the manufacturer, the strongest wavelength of the emission spectrum of the plastic scintillator is approximately 425 nm, and the quantum efficiency of the PMT is as high as 20%. A spectral match could be ascertained between the scintillator and the PMT. The photocathode diameter of the PMT was 5 cm. At both ends of the detector shell, a 5 mm diameter borehole was used as the inlet and outlet of the tritiated water flow to maintain a constant water flow. At the transverse position of the inlet and outlet of tritiated water, a transverse borehole was drilled in the plastic scintillator in the direction parallel to the upper and lower bottom surfaces. At both ends of the plastic scintillator, the parts near the PMT are filled with solidified optically coupled glue to prevent direct contact between tritiated water and the PMT photocathode. Teflon tape was used to seal the ends of the plastic scintillator and the shielding shell.

3 Structure optimization of detector

To ensure that the detector is efficient and has a low minimum detectable concentration, it is necessary to increase the contact area between the tritiated water. The aperture and the number of boreholes, as well as the length of the plastic scintillator, are important factors determining the contact area. At the same time, in the transmission process of scintillation photons, whether or not the inner wall of the borehole is polished also has an important impact on the collection efficiency of scintillation photons. To consider the influence of these factors, we used the Geant 4 software toolkit [19] to simulate the detection of tritiated water concentration using a plastic scintillator.

3.1 Aperture selection of borehole

The range of β-rays generated by tritium decay in water and plastic scintillators is calculated by simulation and β spectral data from Mertens et al. [20]. The calculation results show that 99.4% of the β particles range within 5 μm. β-rays beyond 5 μm from the plastic scintillator hardly contributed to the measurement results. To reduce the calculation time in the program, we set the position of particles in the tritiated water layer within 5 μm from the surface of the plastic scintillator.

To improve the detection efficiency of the system, it is necessary to increase the contact area between the tritiated water and the detector surface. Currently, it is assumed that the detector diameter is 5 cm, and the length is 60 cm. When the aperture is 1 mm, 2 mm, 3 mm, 4 mm, and 5 mm, respectively, and the gap between holes is fixed at

1 mm, the effective emission volumes of the β particles are 0.0050, 0.0051, 0.0034, 0.0032, and 0.0024 L, respectively. When the aperture was 2 mm, the β particle emission volume was the largest. However, owing to the limitations of machine tool technology is easier to drill the drill bit vertically when the aperture is 3 mm. After relevant research on mechanical processing, when the five-axis CNC machine tool uses 3 mm drill bidirectional drilling, it can achieve 60 cm plastic scintillator drilling. Therefore, we determined the detector model as follows: a cylindrical plastic scintillator with a diameter of 5 cm drills the dense boreholes arranged by the array in the direction parallel to the axis, the aperture was 3 mm, and the gap between the holes was 1 mm. The length of the cylindrical plastic scintillator did not exceed 60 cm.

3.2 Construction of detector model and simulation

Based on the parameters in Sect. 3.1, the tritiated water detected by the detector was simulated. In the simulation, the physical process uses the physical process of G4EmLivermorePhysics and the optical physical process of Geant 4 (Optical Physics) [21]. The former is used to solve the transport problem of β particles, mainly providing energy deposition data. The latter can transform energy deposition into optical photons and transport them, and its transport method is based on the theory of geometrical optics. The physical process of G4EmLivermorePhysics is more accurate in simulating low-energy electromagnetic interactions, and its lower energy limit is 100 eV. The electromagnetic interaction processes include Bremsstrahlung, Coulomb scattering, fluorescence effect, and Auger electrons.

The refractive index and absorption length were obtained from the parameters of pure plastic in Ref. [22]. The optical properties of water are taken from the detector parameters of Geant 4's own routine (examples/extended/OpNovice). The quantum efficiency of the PMT adopts the parameters provided by the manufacturer of R6231-100 (http://www.hamamatsu.com.cn/). The detector shell is made of Teflon, the surface of which is a Lambertian reflection [23]. The surface of the detector to Teflon was set as PolishedTeflon_LUT, which is from the measured surface database of Geant 4. In the simulation, the optical surface of each interface was polished.

Electrons are generated in tritiated water and deposited into plastic scintillators to generate photons. Finally, some photons arrive at the PMT to generate photoelectrons. We believe that this is an effective event only when both PMTs output signals simultaneously. Figure 2 shows the photon transport process for the particle deposition energy of the detector. The green line is the transmission path of the scintillation photon, and the gray line at both ends is the

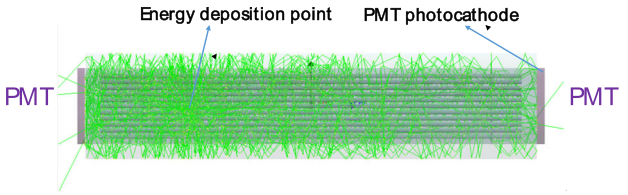

Fig. 2 (Color online) The photon transport process in the detector (green is the transport path of photons)

PMT photocathode. The simulated energy deposition points were marked. The number of photons in the transmission process is lost owing to the self-absorption of the plastic scintillator. In addition, some photons are emitted into the water outside the plastic scintillator and cannot reach the PMT. Therefore, when the energy deposition point was close to the left end, the number of photons transmitted to the right end is less than that to the left end. Therefore, there appears to be a photon flux gradient toward the right in the figure.

3.3 Length selection of plastic scintillator

To realize the measurement of low-concentration tritiated water with 100 Bq/L, the detection system needs to have sufficient detection efficiency, that is, the plastic scintillator should have sufficient contact area with tritiated water. The smaller the aperture, the greater the number of boreholes, and the larger the contact area. However, considering the possible polishing and existing processing level of the borehole in the later stage, we chose the design of a 3 mm aperture and 1 mm gap between holes. Therefore, we can only increase the contact area by increasing the length of the detector and the number of detectors in the detection system. According to the investigation, when two ends of the plastic scintillator are drilled by a five-axis CNC machine tool, 60 cm long drilling can be realized. Therefore, we used Geant 4 to simulate the number of photons received by the PMT photocathode at different lengths (20 cm–60 cm), as shown in Fig. 3.

Figure 3 presents the coincidence photon number spectrum received by the PMT photocathode when plastic scintillators with different lengths measured at the same time. The abscissa is the sum of the number of photons received by the two PMTs when the two PMTs capture no less than one photon at the same time, and the ordinate is the number of times this number appears in the simulation. From Fig. 3, it can be seen that the spectrum of the photon number is similar to the β-ray energy spectrum produced by tritium decay. With the increase in length, the peak position moved to the left. This is because as length increases, the self-absorption effect of the material increases during the transmission of the scintillation

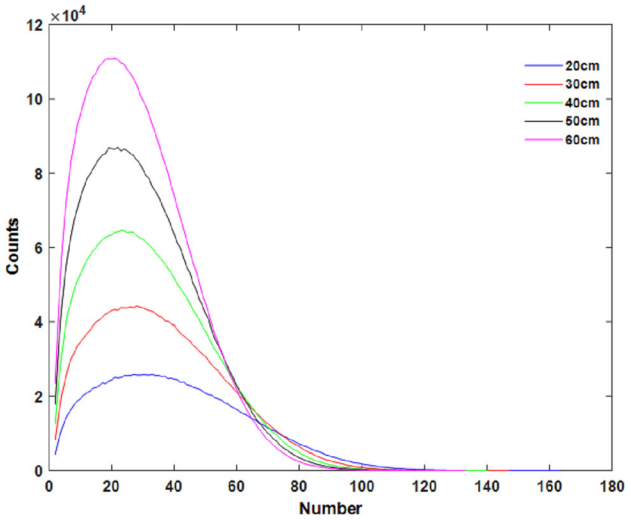

Fig. 3 (Color online) Comparison of coincidence photon number of PMT with different lengths of plastic scintillators

photon. The longer the detector, the longer the path of photon propagation, and the greater the possibility of photons emitting into the outer space of the plastic scintillator in the propagation process. This is another reason why the detection efficiency decreases with an increase in the detector length. This requires a lower noise level and a higher signal-to-noise ratio in back-end electronic devices. However, the β-ray incident on the plastic scintillator in unit time increases linearly with the length, as shown in Table 1. At the same measurement time, according to the number of effective events based on the coincidence photoelectron number, a 60 cm long plastic scintillator captured 3,735,924 times, and a 20 cm long plastic scintillator was captured 1,395,343 times. Using a detector with a length of 60 cm was the optimal choice within the allowable range of the processing level as this saves approximately 2.68 times the measurement time when compared to a 20 cm detector. The detection efficiency in this study is based on the effective emission volumes, and the beta particles generated beyond 5 μm from the surface of the plastic scintillator are not taken into account. The detection efficiency (DE) is the ratio of the number of effective events based on the coincidence photoelectron number to the number of events under certain detection conditions.

$$\mathrm{DE} = \frac{D}{N} \times 100\%,$$

where D is the number of effective events based on coincidence photoelectron number, N is the number of events.

Under the same tritiated water concentration and the same detection time, different sizes of detectors were simulated. When the aperture and the gap between holes are fixed, the length of the plastic scintillator is proportional to the number of electron incidents, which can better observe the relationship between the detection efficiency and length. The probability of particle deposition energy in a plastic scintillator is independent of the detector length. The simulation results are presented in the table below.

When the length of the detector increases from 20 to 60 cm, the detection efficiency of the detector decreases from 4.19 to 3.74% (the quantum efficiency of the PMT is considered in the simulation, that is, when PMTs capture no less than one photoelectron at the same time, we believe that the detector successfully detects an effective case). With an increase in length, the detection efficiency decreases. This is because as the length increases, the self-absorption effect of the material increases during the transmission of the scintillation photon. However, owing to the increase in length, the contact area between tritiated water and the detector increases, and the number of particles incident on the detector per unit time increases. The number of β-rays received by the detector with a length of 60 cm per unit time was three times that of the detector with a length of 20 cm. Using a detector with a length of 60 cm was the optimal choice within the allowable range of the processing level. It saves approximately three times the measurement time compared to a 20 cm detector.

3.4 Study on whether inner wall is polished of borehole

The energy deposited by the β-ray in the plastic scintillator generates scintillation photons, and the scintillation photons propagate in the plastic scintillator to the PMT at both ends. During the propagation of scintillation photons in a plastic scintillator, multiple reflections, refractions, and absorption occur between the tritiated water and the plastic

Table 1 Simulation results

Detector length (cm)	20	30	40	50	60
Number of events	33,333,333	50,000,000	66,666,666	83,333,333	100,000,000
Number of effective events based on coincidence photon number	1,587,340	2,377,602	3,158,911	3,937,217	4,708,828
Number of effective events based on coincidence photoelectron number	1,395,343	2,030,251	2,627,727	3,195,951	3,735,924
Detection efficiency	4.19%	4.06%	3.94%	3.84%	3.74%

scintillator interface. It is great significance to study the influence of the polishing of the inner wall on the number of photons collected by the PMT photocathode. The influence of that on the photon number received by the PMT was simulated using Geant 4. As shown in Fig. 4, the blue line is the photoelectron number spectrum captured by two PMTs at the same time in the case of the ground internal wall of the plastic scintillator, and the green line is the photoelectron number spectrum in the case of the polished internal wall. It can be observed from the figure that when the inner wall is polished, the number of photoelectrons converted by the PMT photocathode was far greater than that when the inner wall was ground. Thus, the detection efficiency of the detector is higher when the inner wall of the plastic scintillator aperture is polished.

3.5 Simulation results

As seen above, when the diameter of the plastic scintillator is 5 cm and the length is 60 cm. The performance of the detector is at its best when 105 boreholes are drilled parallel to the axis, the aperture is 3 mm, the gap between holes is 1 mm, and the inner wall of the borehole is polished. On the left side of Fig. 5, the red line is the normalized distribution of the β-ray energy generated by tritium decay, and the blue line is the normalized distribution of the deposition energy simulated by Geant 4. Because the physical process of G4EmLivermorePhysics has poor simulation accuracy below 1 keV, the curve below 1 keV is abnormal as seen in Fig. 5. From the diagram, it can be found that the peak value of the β-ray produced by tritiated water decay is approximately 3 keV, while the peak value of the deposited energy in the plastic scintillator is approximately 6 keV. The reason for the peak shift to the right is that a part of the relatively high-energy (the right side of the peak) β-rays loses some energy in water before they are incident on the plastic scintillator, and some of the relatively low-energy (the left side of the peak) β-rays are not incident on the plastic scintillator and they lose energy completely. The right figure shows the result obtained by Geant 4 when the length of the plastic scintillator is 60 cm. The red line is the number spectrum of the scintillation photons produced by incident β-rays in a plastic scintillator. The abscissa is the number of scintillation photons, and the ordinate is the number of times the number appears. The green line represents the number of photons captured by a PMT when these photons are simultaneously captured by two PMTs at the same time. The abscissa is the number of photons captured by the PMT, and the ordinate is the number of times the number appears. The blue line represents the spectrum of photoelectrons captured by a PMT when these photoelectrons are captured by two PMTs simultaneously after considering the quantum efficiency of the PMT. The quantum efficiency curve was added to the Geant 4 simulation program by sampling. A total of 100 million β-ray emissions were simulated in tritiated water within 5 μm from the surface of the plastic scintillator. Among them, 4839,367 β-rays deposited energy in plastic scintillation to generate scintillation photons, and the number of photoelectrons captured by PMTs at both ends was 3735,924. In other words, in the effective β-ray emission volume, approximately 4.84% of the β-rays deposit energy in the plastic scintillation to generate scintillation photons, and approximately 77% of the scintillating photons are captured by both ends of the PMT while generating electronic signals. For the effective β-ray emission volume, the detection efficiency (5 μm water layer) of the detector (60 cm long) was approximately 3.74%. Based on this data, we can calculate the number of pulses detected per unit time according to the activity of the β-ray.

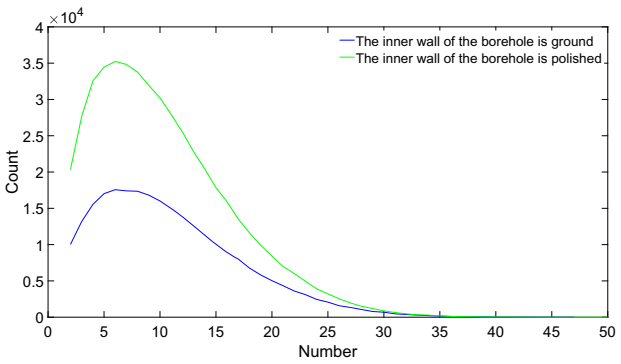

Fig. 4 (Color online) Comparison of coincidence photoelectron number of whether inner wall is polished

Geant 4 was used to simulate a set of detection systems measuring for 3 h. Counting statistics of tritiated water with different activities are shown in Fig. 6. The abscissa in Fig. 6 refers to the number of effective events with different tritiated water activities detected by the detector when measured for 3 h by Geant 4 simulation. The ordinate is the number of times this number appears in the simulation. We simulated 100 million β-rays emission events in the effective volume. It can be seen from Fig. 6 that the number of effective events in tritiated water with different activities is a Gaussian distribution. After calculation, when the activity is from 100 to 10,000 Bq/L, the resolution is 16.13% (16 Bq/L), 7.35%, 5.10%, 3.55%, 2.87%, 2.50%, 2.20%, 2.04%, 1.86%, 1.73%, 1.64%, and 1.50% (150 Bq/L). The detection system can theoretically realize online measurement of tritiated water activity as low as 100 Bq/L. The simulation of the detection system shows that it successfully realizes the online measurement of low-activity tritiated water and reduces the single measurement

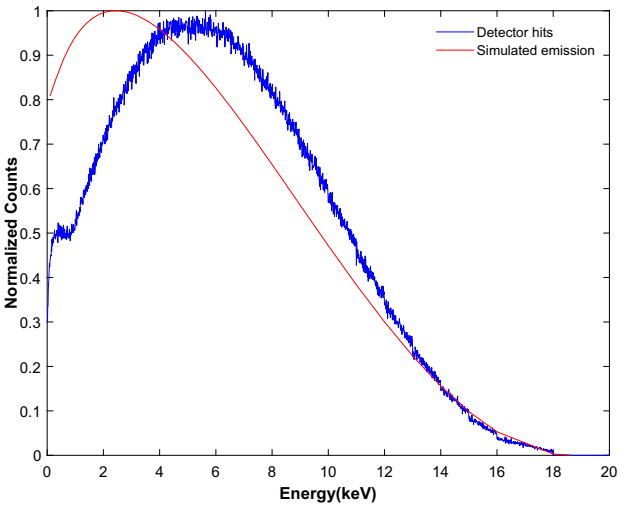

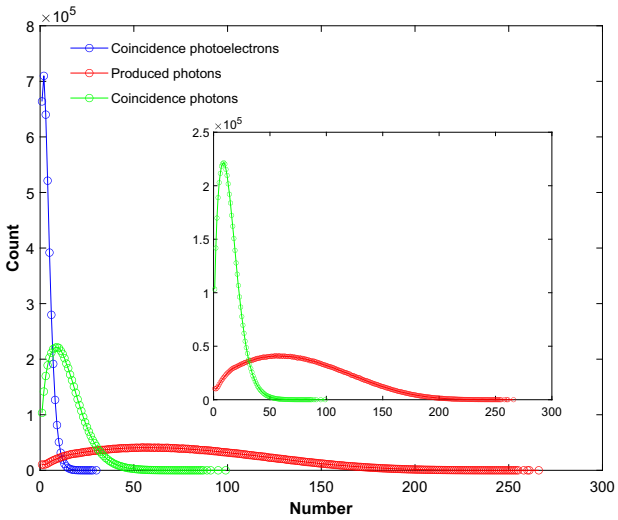

Fig. 5 (Color online) The figure on the left is the normalized energy spectrum. Red is the normalized energy spectrum of β-rays produced by the decay of tritiated water. Blue is the normalized energy spectrum of the deposited energy incident on the plastic scintillator. The figure on the right is the number spectrum of photons and photoelectrons, red is the spectrum of scintillation photons generated by β-ray deposition energy, green is the spectrum of coincidence photons captured by two PMTs, and blue is the spectrum of coincidence photoelectron

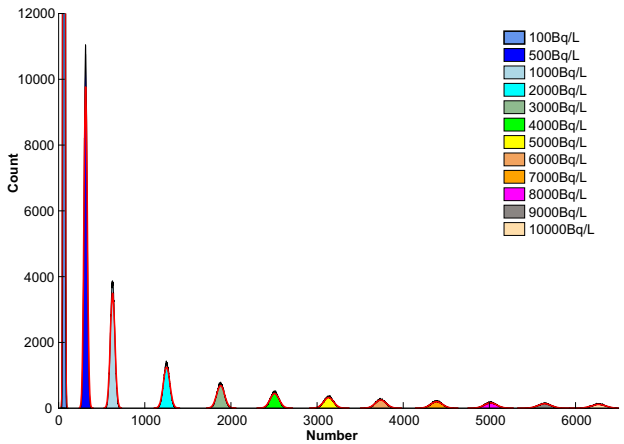

Fig. 6 (Color online) Counting statistics of tritiated water with different concentrations when measured by a single detector in Geant 4 simulation for 3 h

time of the offline liquid scintillation method from to 2–3 days to 3 h.

3.6 Hypothesis of background count and minimum detectable concentration (MDC)

There are several other radionuclides in the liquid effluent of a nuclear power plant, except ^{3}H, like ^{14}C, ^{54}Mn, ^{137}Cs, ^{58}Co, ^{60}Co. The β-ray generated by its decay affects the measurement results. Because the concentrations of ^{54}Mn, ^{137}Cs, ^{58}Co, and ^{60}Co were much lower than ^{14}C, ^{14}C was used as the background source, and the minimum detectable activity concentration (MDC) of the detector was analyzed. The concentration of ^{14}C in the liquid effluent was 37.6 Bq/L. Because the range of rays generated by the decay of ^{14}C is much higher than that of β rays generated by the decay of tritiated water, the effective volume of ^{14}C as the background source is the total volume of tritiated water in the detector (0.42 L). The activities of ^{14}C in the effective volume were calculated to be 15.79 Bq. Assuming that the measurement time is 3 h, the energy spectrum of ^{14}C deposited in plastic scintillator are simulated, and the background count within 0–18.6 keV can be calculated as 118.7. The minimum detectable activity concentration (MDC) applies the formula proposed by Currie in 1968:

$$\mathrm{MDC} = \frac{L_{\mathrm{D}}}{\varepsilon_{\mathrm{m}} I_{\beta} T} \cdot \frac{1}{V} = \frac{2.71 + 4.65\sqrt{B_{\mathrm{t}}}}{\varepsilon_{\mathrm{m}} I_{\beta} T} \cdot \frac{1}{V},$$

where L_{D} (Bq) is the minimum determinable limit; B_{t} is the background count of regions of interest; ε_{m} is the detection efficiency; T (s) is the measuring time; I_{β} is the energy branching ratio corresponding to β-ray; and V (L) is the effective volume of samples. B_{t}=118.7, ε_{m}=3.74%, T = 10,800 s, I_{β}=1. Thus, the minimum detectable concentration was 38.86 Bq/L.

In the liquid effluent of the primary loop of the nuclear power plant, the concentration of ^{14}C as the background source was 37.6 Bq/L. Considering the influence of background counts, the minimum detectable concentration (MDC) of ^{3}H can get to 38.86 Bq/L when the system is detected for 3 h.

4 Other details of the detection system

Because the environment of liquid tritium activity measurement is complicated, the liquid effluent of a nuclear power plant is taken as an example, which also contains the influence of α, γ, high-energy β-rays, and cosmic rays. This method is different from the offline liquid scintillation method. The liquid scintillation method can remove the influence of other rays through physical and chemical methods. To achieve online real-time measurement with this detection system, the energy spectrum of rays in tritiated water must be obtained through back-end electronic devices. However, the detection system cannot identify α, β, and γ rays by waveform [24–26]. Through the analysis and quantitative research of the energy spectrum, we can identify and filter effective low-energy β-rays. In general, it is still necessary to simulate the energy deposition of different rays in the detection system using Geant 4 to provide a basis for later energy spectrum analysis. Finally, the accuracy of the energy spectrum analysis was verified based on the experimental measurement data.

The nuclear power plant needs to sample its liquid effluent regularly and measure its activity using the liquid scintillation method. The detection system can be compared with the liquid scintillation method of measuring the same sample. The accuracy of the energy spectrum analysis method was verified based on the measurement results of the liquid scintillation method. If the energy spectrum analysis scheme cannot achieve a better elimination of the effects of other rays, the liquid to be tested can be purified by an ultrapure water machine to eliminate the effects of other radionuclides. At the same time, the water purification system can eliminate the pollution of plastic scintillators by algae and pollutants in the water to prevent degradation of its detection performance.

Because of the low-energy β-ray deposition energy, the signal amplitude output by the PMT is small, which requires the back-end electronic devices to have large magnification and low noise level, so that the online detection of tritiated water activity based on plastic scintillators can become a reality. Simultaneously, the back-end electronic device designed a mode conversion function. In a later stage, it is necessary to identify the effective low-energy β-ray counts according to the difference in the energy spectrum. According to the collocation of the plastic scintillator and PMT, we use a 500MSPS ADC chip. Because this sampling rate ensures that there are no less than four sampling points at the rising edge, the obtained pulse height can be relatively accurate. In addition, a high sampling rate can greatly reduce the time window of two PMT coincidence judgments, and greatly reduce the probability of false counting of the PMT dark current.

Presently, the processing of the detector and the design of back-end electronic devices have been completed. Electronic devices include two PMT output preamplifiers, a dual-channel 500 MHz sampling data board, and a network communication board. The network communication board corresponds to an IP address. A network communication board can connect five data acquisition boards; that is, an IP address can connect five detectors. Through the switch, a PC can connect multiple network boards, which can double the number of detectors. Today, with the adoption of a bill by the Japanese Cabinet Parliament to discharge radioactive wastewater into the Pacific Ocean, two years later, radioactive wastewater may contain radionuclides such as ^{90}Sr, ^{137}Cs, ^{14}C, and ^{129}I. There are obvious differences between γ-rays and β-rays produced by these major radionuclide decays. The detector system has the function of energy spectrum acquisition. Through in-depth simulation research and energy spectrum analysis, the detection system is expected to become an effective means for online real-time monitoring of multiple particle concentrations in wastewater.

5 Conclusion

This study mainly concluded the following: The range of β-rays produced by tritium decay is within 5 μm in a plastic scintillator and water. Calculations show that when the plastic scintillator's borehole inner wall is polished, the detection efficiency of the detector is higher than that of a detector with a ground inner wall. Through the Geant 4 simulation, when the detector was 5 cm in diameter and 60 cm in length, 105 densely arranged boreholes were drilled parallel to the axis. The aperture was 3 mm and the gap between holes was 1 mm. The detector had the best performance considering the condition of the mechanical processing technology. The simulation shows that when the activity is from 100 to 10,000 Bq/L, the resolution is 16.13% (16 Bq/L), 7.35%, 5.10%, 3.55%, 2.87%, 2.50%, 2.20%, 2.04%, 1.86%, 1.73%, 1.64%, and 1.50% (150 Bq/L). The detection system can theoretically realize online measurements of tritiated water activity to as low as 100 Bq/L. After calculation, when the detector has the optimal performance determined in this paper, the activity of ^{14}C, which is the main background source in the liquid effluent of a nuclear power plant, is 37.6 Bq/L, and the minimum detectable concentration of ^{3}H can reach 38.86 Bq/L in the detection system for 3 h. This study aims to change the current situation in which nuclear power plants can only measure tritiated water activity offline. It provides a real-time online measurement method for tritiated water activity monitoring in nuclear power plants and solves the problem of continuous production of radioactive

waste using the liquid scintillation method. Currently, sewage treatment plants have β-ray activity detection requirements, and the detection system studied has a huge market space. In future nuclear power plants dominated by nuclear fusion reactions, there are more ways to produce liquid tritium and more monitoring points that require online measurement, which enables the detection system's broad application prospects.

Author contributions All authors contributed to the study conception and design. Material preparation, data collection and analysis were performed by Rui-Yang Xu, Chun-Hui Dong, Xiao-Qing Mao, and Qing-Xian Zhang. The first draft of the manuscript was written by Rui-Yang Xu and all authors commented on previous versions of the manuscript. All authors read and approved the final manuscript.

References

1. D.P. Li, Z.Q. Pan, *Radiation Protection Handbook*, 1st edn. (Atomic Energy Press, Beijing, 1990), pp. 118–120. (**in Chinese**)
2. H.B. Ding, N.Y. Wang, *Neutron Source Physics*, 1st edn. (Science Press, Beijing, 1984), pp. 543–544. (**in Chinese**)
3. P.Y. Sun, J.J. Shi, M.Y. Li et al., Accumulation, transference and dynamical disappearance of HTO in simulated marine ecosystem. Acta Sci. Circ. **22**(5), 609-613 (2002). https://doi.org/10.3321/j.issn:0253-2468.2002.05.013 (**in Chinese**)
4. L. Zhu, *Radiochemistry*, 1st edn. (Atomic Energy Press, Beijing, 1985), p. 315. (**in Chinese**)
5. H.Y. Yang, *Tritium Safety and Protection*, 1st edn. (Atomic Energy Press, Beijing, 1997), p. 37. (**in Chinese**)
6. K.J. Hofstetter, H.T. Wilson, Aqueous effluent tritium monitor development. Fusion Technol. **21**, 446–451 (1992). https://doi.org/10.13182/FST92-A29786
7. Council directive 2013/51/euratom. URL https://eur-lex.europa.eu/eli/dir/2013/51/oj
8. F. Liu, Y.H. Li, J. Lin, A hydrogen and oxygen isotope study of groundwater in the yongding river drainage of Beijing and its environmental significance. Acta Geosci. Sin. **29**(2), 161–166 (2008). https://doi.org/10.3321/j.issn:1006-3021.2008.02.005 (**in Chinese**)
9. Y.S. Chai, L.W. Wei, X.G. Kong, Optimization of sample tritium measurement conditions in nuclear power plant primary circuit. Ind. Sci. Trib. **19**(20), 40–41 (2020). (**in Chinese**)
10. M. Matsuyama, Y. Torikai, K. Watanabe, In-situ measurement of high level tritiated water by bremsstrahlung counting. Fusion Sci. Technol. **48**(1), 324–331 (2005). https://doi.org/10.13182/FST48-324
11. M. Matsuyama, M. Hara, Standardization of tritium measuring devices based on a high-sensitivity calorimeter. Fusion Sci. Technol. **54**(1), 182–185 (2008). https://doi.org/10.13182/FST08-A1791
12. M. Matsuyama, K. Takatsuka, M. Hara, Sensitivity of a specially designed calorimeter for absolute evaluation of tritium concentration in water. Fusion Eng. Des. **85**(10), 2045–2048 (2010). https://doi.org/10.1016/j.fusengdes.2010.07.025
13. Y. Hatano, M. Hara, H. Ohuchi et al., Measurement of highly tritiated water by imaging plate. Fusion Sci. Technol. **60**(3), 982–985 (2011). https://doi.org/10.13182/FST11-A12580
14. I. Jakonić, N. Todorović, J. Nikolov et al., Optimization of low-level LS counter quantulus 1220 for tritium determination in water samples. Radiat. Phys. Chem. **98**, 69–76 (2014). https://doi.org/10.1016/j.radphyschem.2014.01.012
15. C. Varlam, I. Stefanescu, O.G. Duliu et al., Applying direct liquid scintillation counting to low level tritium measurement. Appl. Radiat. Isot. **67**(5), 812–816 (2009). https://doi.org/10.1016/j.apradiso.2009.01.023
16. F. Verrezen, H. Loots, C. Hurtgen, A performance comparison of nine selected liquid scintillation cocktails. Appl. Radiat. Isot. **66**(6), 1038–1042 (2008). https://doi.org/10.1016/j.apradiso.2008.02.050
17. Z.L. Chen, S.X. Xing, H.Y. Wang et al., The effect of vial type and cocktail quantity on tritium measurement in LSC. Appl. Radiat. Isot. **68**(9), 1855–1858 (2010). https://doi.org/10.1016/j.apradiso.2010.04.015
18. C.D.R. Azevedo, A. Baeza, E. Chauveau et al., Simulation results of a real-time in water tritium monitor. Nucl. Instrum. Methods Phys. Res. Sect. B **982**, 164555 (2020). https://doi.org/10.1016/j.nima.2020.164555
19. S. Agostinelli, J. Allison, K. Amako et al., Geant4—a simulation toolkit. Nucl. Instrum. Methods Phys. Res. Sect. A **506**(3), 250–303 (2003). https://doi.org/10.1016/S0168-9002(03)01368-8
20. S. Mertens, T. Lasserre, S. Groh et al., Sensitivity of next-generation tritium beta-decay experiments for keV-scale sterile neutrinos. J. Cosmol. Astropart. Phys. **2015**(2), 020 (2015). https://doi.org/10.1088/1475-7516/2015/02/020
21. E. Dietz-Laursonn. Peculiarities in the simulation of optical physics with Geant4. http://arXiv:1612.05162
22. J. Argyriades, R. Arnold, C. Augier et al., Spectral modeling of scintillator for the NEMO-3 and SuperNEMO detectors. Nucl. Instrum. Methods Phys. Res. Sect. A **625**(1), 20–28 (2011). https://doi.org/10.1016/j.nima.2010.09.027
23. X.L. Qian, H.Y. Sun, C. Liu et al., Simulation study on performance optimization of a prototype scintillation detector for the GRANDProto35 experiment. Nucl. Sci. Tech. **32**(5), 51 (2021). https://doi.org/10.1007/s41365-021-00882-2
24. Z. Zuo, H.R. Liu, Y.C. Yan et al., Adaptability of n–γ discrimination and filtering methods based on plastic scintillation. Nucl. Sci. Tech. **32**(3), 28 (2021). https://doi.org/10.1007/s41365-021-00865-3
25. V.M. Thakur, A. Jain, P. Ashokkumar et al., Design and development of a plastic scintillator based whole body β/γ contamination monitoring system. Nucl. Sci. Tech. **32**(5), 47 (2021). https://doi.org/10.1007/s41365-021-00883-1
26. X. Guan, L.Q. Ge, G.Q. Zeng et al., Determination of gross α and β activities in Zouma River based on online HPGe gamma measurement system. Nucl. Sci. Tech. **31**(12), 120 (2020). https://doi.org/10.1007/s41365-020-00828-0